Agricultural and Forest Meteorology 378 (2026) 110956

Contents lists available at ScienceDirect

Agricultural and Forest Meteorology

journal homepage: www.elsevier.com/locate/agrformet

Carbon dioxide dynamics across three stages of tropical peatland conversion to oil palm plantations

Frankie Kiew [a,*], Ryuichi Hirata [b], Takashi Hirano [c], Guan Xhuan Wong [a], Joseph Wenceslaus Waili [a], Kim San Lo [a], Kaido Soosaar [d], Kuno Kasak [d], Ülo Mander [d], Lulie Melling [a]

[a] Sarawak Tropical Peat Research Institute, Lot 6035, Kuching-Kota Samarahan Expressway, Kota Samarahan, Sarawak 94300, Malaysia
[b] National Institute for Environmental Studies, Tsukuba 305-8506, Japan
[c] Research Faculty of Agriculture, Hokkaido University, Sapporo 060-8589, Japan
[d] University of Tartu, Vanemuise 46, Tartu 51014, Estonia

ARTICLE INFO

Keywords:
CO_2
Eddy covariance
Land conversion stages
Near-ground environmental conditions
Net ecosystem exchange
Tropical peatlands

ABSTRACT

This study represents the first long-term investigation spanning from a tropical peat swamp forest (PSF) to its conversion into an oil palm plantation (OPP), offering valuable data for assessing carbon dioxide (CO_2) dynamics across different conversion stages. The conversion of tropical peat swamp forests to oil palm plantations has significant implications for CO_2 dynamics. However, ecosystem-scale studies investigating CO_2 dynamics across different stages of land conversion are lacking. This study used the eddy covariance (EC) technique to measure the net ecosystem exchange (NEE) of CO_2 above a tropical peat swamp forest in Sarawak, Malaysia, from 2011 until it was cleared in 2017 and ultimately converted into an OPP in 2018. Our study found that the removal of forest biomass during land preparation led to a substantial increase in annual NEE from 25 ± 179 (2011 to 2016) to 2732 ± 655 g C m^{-2} $year^{-1}$ (2017 to 2019). This increase was attributed to an 83 % reduction in gross primary productivity (GPP) and a 14 % reduction in ecosystem respiration (R_{eco}). The near-ground environmental conditions also significantly changed across the conversion stages, inducing drier conditions compared to the forest. These changes were found to affect the controlling factors of nighttime NEE during conversion, resulting in a negative relationship with both air temperature and vapor pressure deficit above canopy, in contrast to the typical relationship with groundwater level observed before conversion. The conversion is also found to cause significant reduction in overall ecosystem photosynthetic activity as evidenced by the reduction in maximum gross photosynthetic rate (P_{max}), photosynthetic photon flux density (PPFD), quantum yeild (α), and dark respiration (RE_d). Although ecosystem-scale assessments of CO_2 dynamics provide insights into how ecosystems respond to changes in relation to land conversion, it is crucial to assess other respiration components, such as soil respiration and aboveground woody debris, for a more comprehensive analysis.

Introduction

Tropical peatlands can take over millennia to form and contain approximately 105 Pg of carbon (C) stock based on recent estimates, corresponding to 17 % of the total global peat C (Dargie et al., 2017; Page et al., 2011). In Southeast Asia, a large amount of peat C (68.5 Pg) is mainly concentrated in Indonesia and Malaysia (Page et al., 2011). This ecosystem is a unique and important C stock because of the coexistence of tropical rainforests and C-rich peat. The aboveground biomass (AGB) of peat swamp forest (PSF) can reach up to 500 Mg C ha^{-1} (Waqar et al., 2020). Over the past few decades, PSF has been converted into both small-scale and industrial plantations, especially for oil palms. The oil palm (*Elaeis guineensis* Jacq.) is regarded as an economically efficient oil crop because of its high yield and cost-effectiveness (Dislich et al., 2017). Indonesia and Malaysia contribute about 85 % of the global production of palm oil, and their global demand is expected to double by 2030 compared to 2010 (Yan, 2017). The need for economic growth through agricultural development is one of the factors that lead to land conversion in developing countries. Due to the large C stock, conversion of PSF often triggers environmental issues associated with C emissions to

* Corresponding author.
E-mail address: frankiek@sarawak.gov.my (F. Kiew).

https://doi.org/10.1016/j.agrformet.2025.110956
Received 3 April 2024; Received in revised form 29 June 2025; Accepted 21 November 2025
Available online 2 December 2025

the atmosphere in the form of CO_2. Houghton and Goodale (2004) concluded that the highest C fluxes arise from the clearing of forests for croplands due to the higher C stock per hectare of trees as compared to crops, and 25-30 % C loss from topsoil following cultivation. In addition, changes in land use have the potential to double GHG emissions compared to intact PSF ecosystems (Deshmukh et al., 2023). Its high C stock is highly sensitive to hydrological changes as compared to temperate or boreal peatlands, which can significantly enhance CO_2 emissions from elevated peat decomposition. The woody and lignin-rich characteristics of tropical peat also makes it challenging to compare emissions profile and C dynamics of those of boreal and temperate peatlands.

Preceding PSF reclamation, groundwater level (GWL) lowering through drainage is crucial in aiding peat mechanical compaction to increase peat soil bulk density, soil surface load-bearing capacity, and micropores (Melling et al., 2005a, 2005b, 2008). However, GWL lowering has been claimed to cause peatlands to shift from C sinks to C sources through the increase in CO_2 deposition to the atmosphere, but methane (CH_4) emissions are expected to be lowered (Couwenberg, 2011; Furukawa et al., 2005; van Huissteden et al., 2006). However, GWL management and peat compaction could reduce C emissions from peat soil in the oil palm plantation (OPP) (Ishikura et al., 2018). In addition, our previous paper (Wong et al., 2020) reported a significantly lower CH_4 emission in an OPP as compared to undrained PSF (2.19 $\pm$ 0.21 vs. 8.46 $\pm$ 0.51 g C m^{-2} $year^{-1}$, respectively) in Sarawak, because a low GWL provides favorable conditions for oxidative peat decomposition but is disadvantageous for methanogenesis (Hirano et al., 2009; Melling et al., 2005a). This is associated with enhanced microbial degradation of organic matter in the soil, as also observed in boreal and temperate peatlands (Jaatinen et al., 2008; Laiho, 2006). CO_2 emissions through peat decomposition were estimated between 27.3 Mg C ha^{-1} $year^{-1}$ and 48.5 Mg C ha^{-1} $year^{-1}$ following drainage as reported by Hooijer et al. (2012) using 25-year-long subsidence data. In addition, Miettinen et al. (2017) reported CO_2 emissions from peat oxidation in insular Southeast Asia in 2015 of up to 64 Mg C $year^{-1}$ in industrial plantations. Our previous study (Kiew et al., 2020) over a 7 to 10-year--old OPP showed an average annual net ecosystem CO_2 exchange (NEE), of 9.94 $\pm$ 1.58 Mg C ha^{-1} $year^{-1}$ over a 4 years period, which was mainly caused by a reduction in gross primary production (GPP), induced by high tree mortality and toppling. However, R_{eco} is comparable to that of secondary PSF (Kiew et al., 2017). In this paper, we also highlight the possibility of large emissions from the decomposition of former forest remnants in the form of plant debris.

The diurnal and seasonal variability of environmental conditions of an ecosystem is strongly influenced by topography and vegetation cover. For instance, the air temperature of an OPP can reach up to 2.8°C higher than nearby tropical forests (Luskin and Potts, 2011). The leaf area index (LAI) plays an important role in microclimate processes rather than regulating environmental variability (Hardwick et al., 2015). We found in our previous study that even a mature OPP has a lower LAI than a secondary PSF, mainly because of the high mortality rate and toppling (Kiew et al., 2017, 2020). Important ecosystem processes, such as canopy interception, evapotranspiration, and gross photosynthesis, are directly affected by LAI because leaf surfaces constitute the primary frontier of energy and mass exchange. During land clearing, a significant loss of vegetation cover is expected, and a low LAI is expected during the early stage of OPP establishment. These conditions can significantly alter the microclimate, thus disrupting the ecosystem's CO_2 balance.

To date, published data on ecosystem-scale CO_2 balance during the conversion stages of tropical peatland to OPP are scarce. Therefore, we presented a 9-years CO_2 flux data measured using the eddy covariance technique above a PSF in Sarawak, Malaysia. During the study period, PSF was converted into an industrial OPP. Therefore, the CO_2 balance before, during and after the conversion can be assessed. This study aims to (1) quantify the NEE across conversion stages, (2) examine changes in environmental conditions, and (3) discuss how CO_2 dynamics respond to changes in environmental conditions.

Material and methods

Study site and land-use descriptions

Flux measurements were carried out at the tropical peatland ecosystem located in the Sri Aman division of Sarawak, Malaysia (1°23′59.42″ N, 111°24′6.69″ E). The study site was formerly a secondary tropical peat swamp forest (Kiew et al., 2017), with estimated aboveground biomass of 70.9, 72.5, and 66.6 tC ha^{-1} in 2015, 2016, and 2017, respectively. Tree densities were 2027 and 1685 trees ha^{-1} in 2016 and 2017, respectively. The dominant tree species were *Litsea sp.* and *Aglaia spp* (Fig. 1A). In 2017, the forest was converted to an OPP. Land clearing was visible from the flux tower during a site visit on 26th June 2017 (Fig. 1B).

All aboveground biomass (AGB) within the flux footprint area was cleared in August 2017, although land clearing activities began as early as March 2017. Oil palm trees were planted in April 2018, with fresh fruit bunches harveting starting in 2020. Therefore, the period before land conversion was defined as the period before 1st March 2017. The period during conversion was defined as the period from 1st March 2017 to 30th April 2018, and the period after conversion was defined as the period from 1st May 2018 to December 2019 (Table 1). The term "land use" and "conversion stage" will be used interchangeably in this article.

Prior to planting, the tree biomass was partially burned, and the remains were stacked in rows, known as stacking rows. Then, the GWL was lowered through the construction of water gates and ditches before mechanical compaction of the peat was conducted. Peat compaction aims to increase the bulk density of peat soil, which can benefit both plant growth (avoid leaning and toppling) and prevent peat fires (increase moisture holding capacity). Peat depths measured at random locations (single point) near the flux tower were 9.8 and 7.4 m in 2010 and 2011, respectively. Following land clearing and mechanical compaction, peat depth was measured between 5.4 and 7.2 m in 2018.

Flux and environmental variables measurement

The CO_2 flux measurement was conducted from 2010 to the present, but the data presented in this article only cover the period from 2011 to 2019. At the beginning of the measurement, CO_2 flux was measured at a height of 41 m (Kiew et al., 2017) before changing to 21 m in November 2017, after considering the changes in the height of the vegetation cover. We utilized a sonic anemometer/thermometer (CSAT3, Campbell Scientific Inc., Logan, UT, USA) in conjunction with an open-path CO_2/H_2O analyzer (LI7500A, Li-Cor Inc.) to measure three-dimensional wind velocity, air temperature, CO_2 density, and water vapor density at a frequency of 10 Hz. The CO_2 concentrations measurement heights to calculate CO_2 profile, using a closed-path CO_2 analyzer (LI820; LI-COR Inc.), were also changed from the heights of 41, 21, 11, 3, 1, and 0.5 m to 21, 11, 5, 3, 1, and 0.5 m. Environmental variables measurements were similar to Kiew et al. (2018), encompassing four components of solar radiation, photosynthetic photon flux densities (PPFD), wind speed and direction, air temperature at two heights (T_{air}_1; 41/21 m and T_{air}_2; 3 m) and relative humidity (RH_1; 41/21 m and RH_2; 3 m), volumetric water content at 2 depths (VWC_1; 0 - 10 cm and VWC_2; 0 - 30 cm), soil temperature at 2 depths (T_{soil}_1; 5 cm and T_{soil}_2; 10 cm), GWL, and precipitation. Due to large gaps in precipitation data, the missing monthly precipitation data were filled using monthly precipitation data obtained from a meteorological station approximately 26 km from the flux tower (Lingga station). Similar to eddy flux measurements, RH and T_{air} above the canopy were also measured at a height of 41 m before the land conversion but moved to 21 m in November 2017. The RH and T_{air} below the canopy were maintained at a height of 3 m throughout the study period. The half-hourly vapor pressure deficit at two heights (VPD_1; 41/21 m and VPD_2; 3

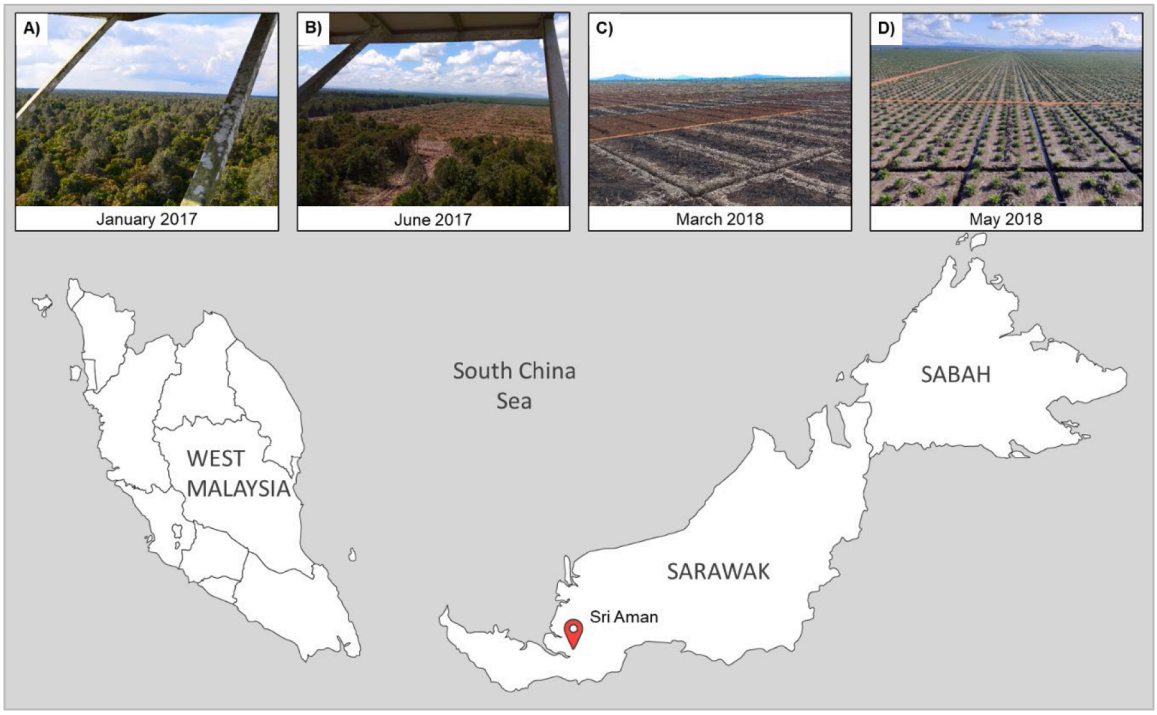

Fig. 1. Location and flux tower view of the study site: A) January 2017, B) June 2017, C) March 2018, and D) May 2018. Land clearing was visible from the tower site in June 2017. Controlled burning was done in February 2018.

Table 1
Period definitions for the conversion stages.

Conversion stage	Land use type	Date
Before conversion	Secondary Forest	1st January 2011 to 28th February 2017
During conversion	Cleared land	1st March 2017 to 30th April 2018
After conversion	Young plantation	1st May 2018 to 31st December 2019

m) was calculated using the measured RH and T_{air}.

Flux processing, quality control and gap-filling

The CO_2 flux half-hourly data (2011–2019) were processed with Flux Calculator software Version 2.0 (Ueyama et al., 2012) which included spike removal, planar fit rotation, frequency response correction, and air density fluctuation correction. The CO_2 storage change below the eddy sensors was estimated half-hourly from the temporal changes in CO_2 profiles. Finally, the sum of the eddy CO_2 flux and CO_2 storage change was calculated as net ecosystem CO_2 exchange (NEE).

Data quality control was performed using a method similar to that described by Kiew et al. (2018). NEE was filtered out based on its deviation from the mean diurnal variation ± 3 standard deviations (SDs) calculated using 13 days moving window. Second, the mean absolute deviation (MAD) spike detection method (Papale et al., 2006) was applied for NEE data screening. Friction velocity (u^*) filtering was applied to the nighttime NEE (PPFD $\leq$ 10 μmol m^{-2} s^{-1}) using u^* threshold estimated with the Flux Analysis Tool software (Ueyama et al., 2012). The u^* threshold was estimated at 0.16 and 0.12 m s^{-1} before and after conversion, respectively.

Data gaps were inevitable owing to both instrument malfunctions and occasional power outages. There was also a huge data gap from August 2015 to February 2016 due to several occurrences of power supply interruptions. The initial data loss rate due to technical issues in the field was 51.1 %. The remaining 1.6 % was removed due to rain events, and 15.1 % was removed by u^* filtering. Only 31.1 % of the data survived quality control using MAD and mean diurnal variation filtering. Therefore, missing NEE data were filled out using the marginal distribution sampling (MDS) method (Reichstein et al., 2005). We adopted the same configurations for MDS gap filling as in Kiew et al. (2018) for period before conversion and after conversion. Given the distinct responses of NEE to environmental factors across different land-use stages (before, during, and after conversion), the data for each period were treated as separate datasets during the gapfilling using lookup table in MDS. The missing daytime NEE for all periods were "looked up" based on similar environmental conditions of ± 25 μmol m^{-2} s^{-1} for PPFD, ± 1.0°C for T_{air}_1 and ± 0.2°C for T_{soil}_2. For the nighttime NEE before and after conversion, GWL (± 2.5 cm), VWC_1 (± 0.05 m^3 m^{-3}) and T_{soil}_2 (± 0.2°C) were used, while T_{air}_1 (± 1.0°C) and T_{soil}_2 (± 0.2°C) were used for the conversion period. The same lookup table algorithm for MDS gap filling was used to extrapolate nighttime NEE into daytime R_{eco}. GPP was assumed to be zero at night, and R_{eco} was equivalent to nighttime NEE. Gaps in environmental variables were filled using the mean diurnal variation (MDV) method. Due to the lack of data availability, half-hourly GWL was partly filled by the neural network method (*caret* package in R software version 3.6.3) using GWL measurements at a nearby forest (approximately 10 km away from the flux tower).

Statistical analysis

All statistical analyses in this study were performed using R Statistical Software version 4.0.2 (R Core Team, 2020). The mean comparison of the daily maximum and minimum of T_{air}, VPD, VWC, and T_{soil} among conversion stages was analyzed using the ANOVA test. Then, the differences between means were identified using Tukey's honestly significant difference (HSD) method. The same statistical approach was applied to compare the means of monthly gap-filled NEE, R_{eco}, and GPP across conversion stages.

The photosynthetic parameters were obtained through optimizing a non-linear least squares fitting of the non-rectangular hyperbola function, as described by Kiew et al., (2018). The light-response function was fitted, and the daily parameters were estimated using a sliding window approach, employing a window size of 14 days (672 observations) with an increment of 1 day (48 observations). Subsequently, the Welch Two-Sample t-test methodology was employed to assess the difference in the means of these parameters before (PSF) and after conversion (OPP). The period during conversion was excluded due to the absence of vegetation cover.

Results

Environmental conditions following land conversion

The temporal variation of precipitation at the study site was obscure; however, relatively large precipitation can often be observed between November and January (Fig. 2A). The mean ± 1SD of monthly precipitation was 216 ± 109 mm month^{-1} with a maximum of 526 mm month^{-1} recorded in December 2013 and a minimum of 20 mm month^{-1} in July 2011. In the 9-year period, monthly precipitation fell below the 100 mm month^{-1} threshold for tropical dry months (Malhi et al., 2002) in 19 occurrences. The highest precipitation was normally recorded between October and March every year, which resulted in a high cloud cover that led to a relatively lower PPFD during the period. This led to an annual precipitation of 2665 ± 320 mm year^{-1}; the maximum was recorded at 3240 mm year^{-1} in 2017, while the minimum was 2120 mm year^{-1} in 2014. The monthly precipitation displayed a decreasing trend starting in February 2019, reaching a value of less than 100 mm month^{-1} in April, and this trend persisted until September 2019. Despite the dry weather conditions, GWL only began to decrease after May 2019.

On a monthly basis, GWL fluctuated between -139.2 cm to 4.6 cm throughout the study period (Fig. 2B); mean ± 1SD were -19.2 ± 17.4 cm, -102.1 ± 31.6 cm, -105.3 ± 17.9 cm respectively for each land uses. Monthly GWL started to decrease in March 2017 to -61.1 ± 16.2 cm in April 2017. The lowest GWL during conversion could be due to the construction of a drainage system prior to land preparation, and water control via water gates upon plantation establishment. However, since December 2018, the GWL was maintained above -90 cm through the

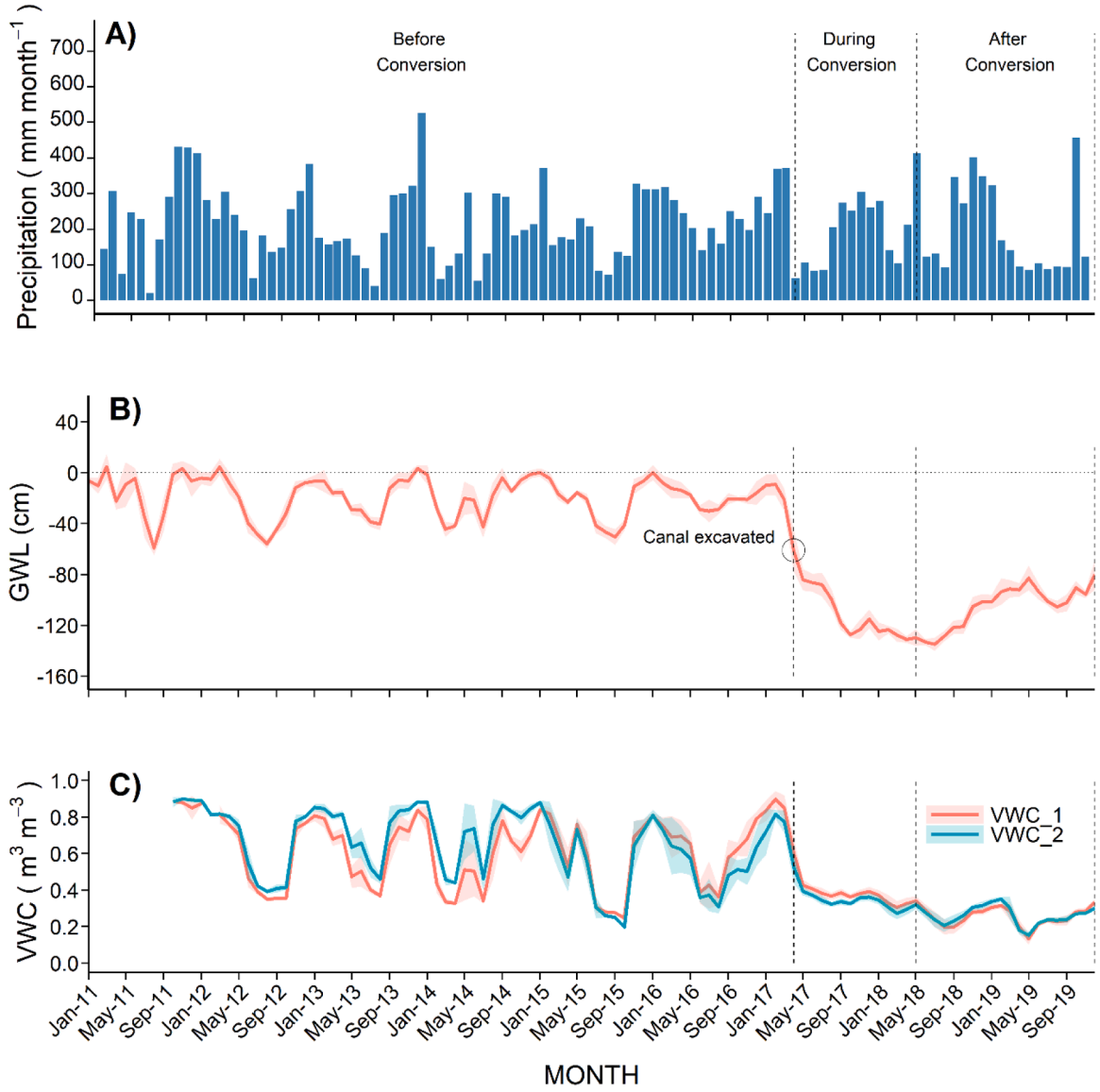

Fig. 2. Monthly variation of hydrological variables from 2011 to 2019: A) total precipitation, B) GWL, and C) VWC: VWC_1, measured at a depth of 0 – 10 cm, and VWC_2 at a depth of 0 – 30 cm depth. Solid coloured lines denote the monthly means of daily values and shaded areas are the standard deviations. Dotted vertical lines indicate borders between conversion stages.

drainage system, supported by substantial precipitation exceeding 250 mm month^{-1} from September 2018 to January 2019.

Before conversion, the temporal variation in VWC exhibited a pattern similar to that observed in the monthly GWL (Fig. 2C). However, after December 2018, there was no significant increase in VWC recorded, despite the GWL increasing above -90 cm. A significant positive linear relationship between monthly GWL and VWC was observed only when the GWL was above -60 cm ($R^2 > 0.84$, $p < 0.01$). As shown in Table 2, both the daily maximum and minimum VWC at both depths decreased significantly during conversion, and this reduction persisted even after conversion. The lack of shading from the dense canopy may have suppressed the moisture retention capability of the topsoil associated with the high exposure to solar radiation, as evidenced by the increase in T_{soil} and midday albedo (Fig. 3A&D) following conversion. Furthermore, both the daily maximum and minimum T_{soil} significantly increased ($p < 0.05$, Table 2) from before conversion to during conversion, and further increased from during conversion to after conversion. Albedo serves as a common indicator for evaluating the potential occurrence of topsoil drying (Gascoin et al., 2009; Idso et al., 1975), given its sensitivity to changes in the soil moisture content and surface properties. On a daily basis, the mean midday albedo (10:00 to 14:00 hours) was significantly different between periods ($p < 0.01$); it was the highest after conversion, followed by during conversion and before conversion.

As shown in Fig. 3A&C, the monthly T_{air} showed a parallel trend with PPFD but was negatively correlated with precipitation ($p < 0.05$). Before conversion, T_{air}_2 (below the canopy) was lower than T_{air}_1 (above the canopy). However, after March 2017, T_{air}_2 significantly increased to a value higher than T_{air}_1. As shown in Table 2, both the daily maximum and minimum T_{air}_1 values decreased during conversion but increased after conversion to match those before conversion. In contrast, the daily maximum and minimum values of T_{air}_2 increased significantly from the period before conversion through the period during conversion to the period after conversion. Both the daily maximum and minimum values of T_{air}_1 were higher than those of T_{air}_2 before conversion. Following conversion (during conversion and after conversion), T_{air}_2 increased to a higher magnitude than T_{air}_1. The daily maximum of VPD_1 and VPD_2 increased from the period before conversion to the period during conversion, and further increased after conversion. However, the daily minimum increased significantly after conversion. During conversion, the daily minimum was statistically indistinguishable. The middday VPD above the canopy (VPD_1) was higher than VPD_2 before conversion but decreased to lower than VPD_2 during conversion (Fig. 3B). However, the difference in vertical profile was not observed after conversion.

Temporal and interannual variation of CO_2 fluxes

Fig. 4 shows the temporal variation in the monthly NEE from January 2011 to December 2019. Before conversion, the mean of monthly NEE was slightly negative at -3 ± 86 g C m^{-2} month^{-1}. Throughout this period, the monthly NEE remained mostly below zero, except for the period from September 2015 to February 2016 (Fig. 4). The high value of NEE during this period probably arises from gap-filling biases and uncertainties due to the long gaps in both measured NEE and meteorological data caused by power supply interruptions. This elevated monthly NEE led to a high annual NEE in 2015, as shown in Table 3 (244 g C m^{-2} year^{-1}). During conversion, the monthly NEE increased drastically to 232 ± 60 g C m^{-2} month^{-1} (Fig. 5), with the highest value recorded at 330 g C m^{-2} month^{-1} in October 2017. This large positive NEE persisted until after plantation establishment in May 2018 (after conversion), with the monthly NEE recorded at 261 ± 60 g C m^{-2} month^{-1}. In most months, the NEE was below 300 g C m^{-2} month^{-1}. However, there was a sudden spike of 576 g C m^{-2} month^{-1} observed in August 2018, likely associated with burning near the flux tower. Judging from the Fused AHI-VIIRS based fire Emissions (FAVE) data (Lu et al.,

Table 2
Means of daily maximum and daily minimum of environmental variables in each conversion stages (mean ± 1 standard deviation (SD)).

Conversion Stage	T_{air}_1 (°C)		T_{air}_2		VPD_1 (kPa)		VPD_2		T_{soil}_1 (°C)		T_{soil}_2		VWC_1 (m^3 m^{-3})		VWC_2	
Daily maximum:																
Before conversion	31.2	± 1.7^a	30.9	± 1.8^a	1.37	± 0.56^a	1.07	± 0.57^a	23.0	± 1.2^a	22.5	± 1.0^a	0.63	± 0.05^a	0.66	± 0.05^a
During conversion	30.5	± 1.8^b	31.7	± 1.8^b	1.47	± 0.50^b	1.51	± 0.50^b	24.7	± 1.6^b	24.7	± 1.0^b	0.38	± 0.19^b	0.34	± 0.19^b
After conversion	31.2	± 1.7^a	32.1	± 1.7^c	1.63	± 0.50^c	1.61	± 0.50^c	26.6	± 0.6^c	25.9	± 0.6^c	0.27	± 0.07^c	0.27	± 0.07^c
Daily minimum:																
Before conversion	23.5	± 0.7^a	23.1	± 1.2^a	0.01	± 0.15^a	0.00	± 0.01^a	21.9	± 1.0^a	22.0	± 0.7^a	0.60	± 0.04^a	0.64	± 0.03^a
During conversion	23.0	± 1.1^b	23.6	± 0.9^b	0.02	± 0.04^a	0.00	± 0.14^a	23.1	± 1.0^b	23.6	± 0.8^b	0.34	± 0.19^b	0.31	± 0.20^b
After conversion	23.5	± 0.9^a	24.7	± 0.7^c	0.06	± 0.03^b	0.04	± 0.00^b	23.5	± 0.6^c	23.6	± 0.7^b	0.24	± 0.06^c	0.25	± 0.05^c

T_{air}_1 and T_{air}_2 were measured above and below canopy respectively (refer to Material and methods for the measurement heights across conversion stages, heights were similar for VPD_1 and VPD_2). T_{soil}_1 and T_{soil}_2 were measured at depths of 5 and 10 cm, respectively. VWC_1 and VWC_2 were measured at depths of 0 – 10 and 0 – 30 cm, respectively.
Significant differences ($p < 0.05$) among values in each column are denoted by distinct letters, as determined by Tukey's Honestly Significant Difference (HSD) test.

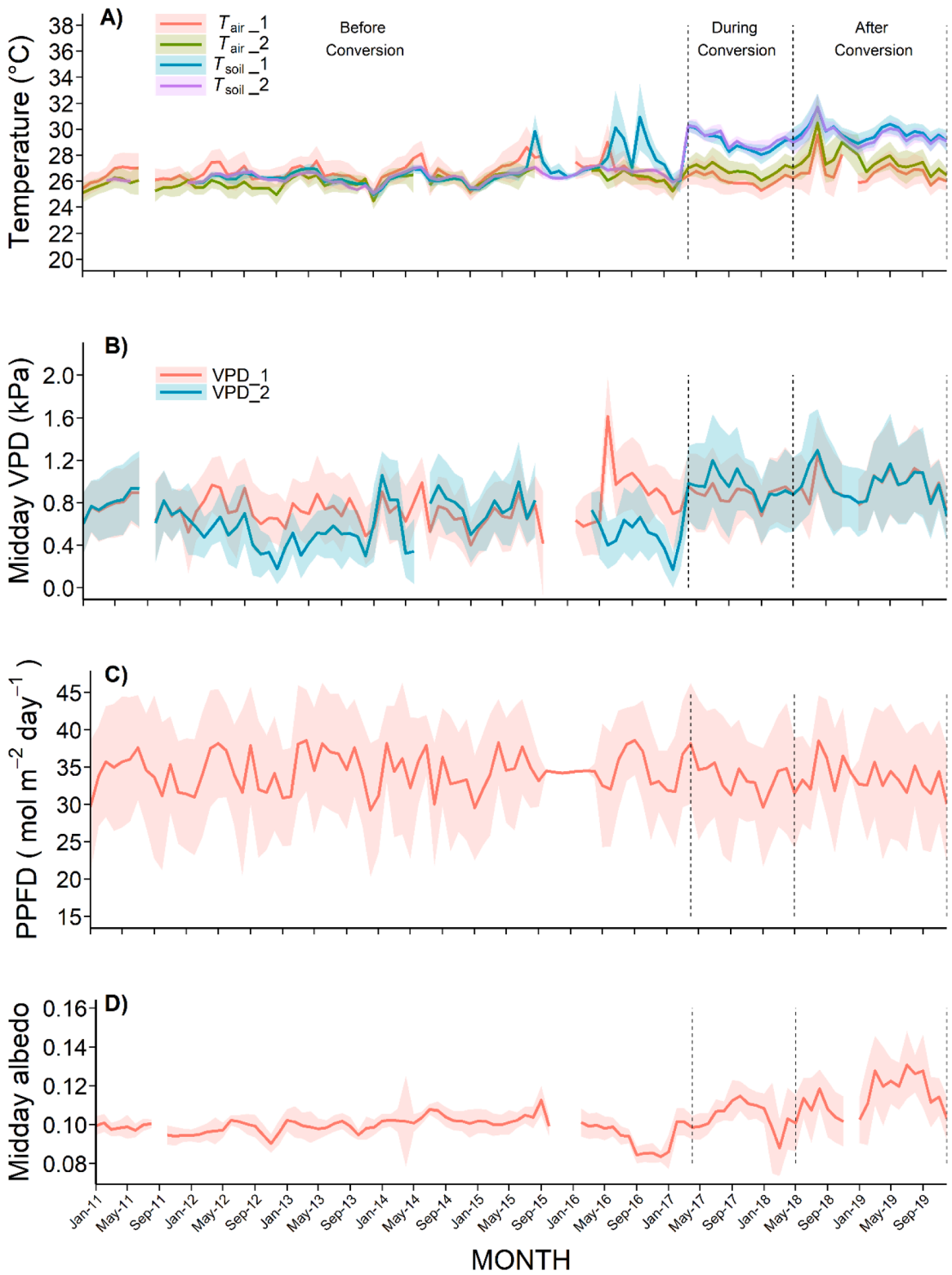

Fig. 3. Monthly variation of environmental variables from 2011 to 2019: A) temperature, B) midday VPD, C) PPFD, and D) midday albedo (PPFD > 10 μmol m^{-2} s^{-1}) of shortwave radiation. The midday values were calculated between 10:00 to 14:00 hours. Solid coloured lines denote the monthly means of daily values and shaded areas are the standard deviations. Dotted vertical lines indicate borders between conversion stages.

2023) in 2018, several fire events were detected within the plantation area during that period.

A mean comparison of the mean monthly NEE, R_{eco}, and GPP was used to assess the changes in CO_2 fluxes across the conversion stages (Fig. 5). Due to the absence of the biomass required for GPP, NEE was not partitioned into R_{eco} and GPP during conversion. The removal of forest biomass during conversion increased the monthly NEE drastically from -3 ± 86 g C m^{-2} month^{-1} before conversion to 232 ± 39 g C m^{-2} month^{-1} during conversion. Conversely, NEE further increased to 261 ± 60 g C m^{-2} month^{-1} after conversion. When comparing the R_{eco} before

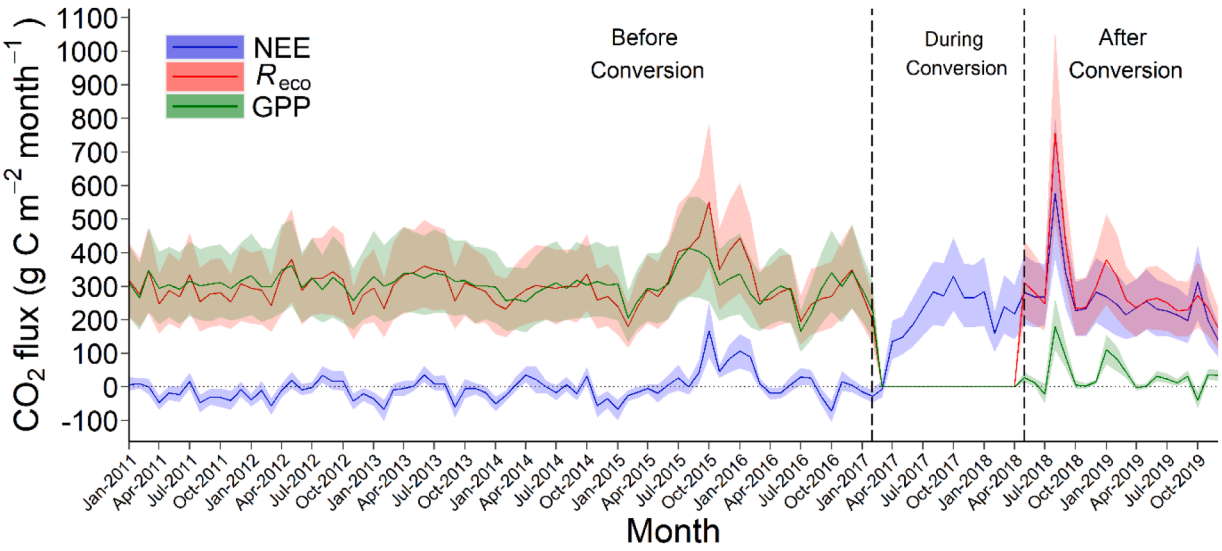

Fig. 4. Monthly sum of NEE (blue), R_{eco} (red), and GPP (green). The uncertainties (95 % confidence intervals) for the monthly fluxes were estimated using block bootstrapping method, with 1000 resampling. A block size of 48 (number of half-hourly data in a day) was used to ensure that the temporal structure is preserved. The uncertainties are depicted as shaded areas around the monthly sums. Dotted vertical lines indicate borders between three conversion stages.

Table 3
Annual values of NEE, R_{eco}, GPP, GWL, VWC, and precipitation from 2011 to 2019 on a calendar basis. R_{eco} and GPP were not calculated for 2017 and 2018, as this period includes the during conversion stage which NEE partitioning was not performed.

Year	NEE (gC m^{-2} yr^{-1})	R_{eco}	GPP	GWL (cm)	VWC (m^3m^{-3})	Precipitation (mm yr^{-1})
2011	-207	3450	3657	-15.0	0.87	2965
2012	-98	3633	3731	-22.8	0.60	2729
2013	-140	3708	3848	-17.0	0.64	2563
2014	-100	3392	3492	-20.3	0.55	2120
2015	244	4102	3858	-23.2	0.57	2603
2016	152	3545	3393	-18.1	0.62	2732
2017	2072	-	-	-78.7	0.52	3240
2018	3382	-	-	-123.6	0.28	2381
2019	2743	3116	373	-94.1	0.25	2656
Mean ± 1 SD	894 ± 1424	3564 ± 305	3193 ± 1255	-45.9 ± 41.4	0.54 ± 0.19	2665 ± 320

and after conversion (forest vs. oil palm), its respective means of 301 ± 60 and 296 ± 123 g C m^{-2} $month^{-1}$ were statistically indistinguishable ($p > 0.05$). On the other hand, monthly GPP significantly reduced from 303 ± 40 to 34 ± 50 g C m^{-2} $month^{-1}$, after conversion.

The annual NEE, R_{eco}, and GPP before conversion were analyzed based on data from 2011 to 2016. Before conversion, the annual NEE, R_{eco}, and GPP were -25 ± 179, 3638 ± 255, and 3663 ± 189 g C m^{-2} $year^{-1}$, respectively (Table 3), indicating a net CO_2 sink. However, the annual NEE during conversion, estimated using the monthly NEE over a 12-month period from May 2017 to April 2018 was 2460 g C m^{-2} $year^{-1}$, indicating a net CO_2 source to the atmosphere. R_{eco}, and GPP in 2017 and 2018 were also not calculated because R_{eco}, and GPP were not estimated during conversion. After conversion, complete 1-year data were available only for 2019, during which the mean annual values of NEE, R_{eco}, and GPP were 2743, 3116, and 373 g C m^{-2} $year^{-1}$, respectively. As shown in Fig. 6, the cumulative sum of NEE before conversion was negative, indicating that the ecosystem was a net C sink. However, the NEE became more positive following land conversion and reached 8048 g C m^{-2} at the end of the study period, indicating a net C source.

CO_2 fluxes response to environmental variables

The response of the half-hourly nighttime NEE (R_{eco}) to the environmental variables was analyzed using the non-gap-filled nighttime NEE (Table 4). Before conversion, the nighttime NEE was negatively correlated with GWL, VWC_1, and VPD ($p < 0.05$) but positively correlated with T_{soil}_2 ($p < 0.05$), with the relationship with GWL being the strongest (r = -0.06, $p < 0.01$). In contrast, during conversion, nighttime NEE exhibited a negative relationship with T_{air} and VPDs (both heights) and a positive relationship with GWL. Despite the relatively smaller sample size compared to before conversion, these relationships were relatively stronger, as evidenced by the smaller p-value. The strongest correlation was observed with VPD_1 (r = -0.24, $p < 0.01$). However, the response of nighttime NEE after conversion was comparable to that before conversion, as GWL became the strongest controlling factor (r = -0.09, $p < 0.01$, $R^2 = 0.009$), followed by VWC_1, T_{soil}_2, and T_{air}_1.

The mean comparison of light response parameters before and after conversion reveals notable changes in P_{max}, α, and RE_d. Following the conversion, all three parameters exhibit significant decreases ($p < 0.001$, Table 5). Specifically, the mean P_{max} decreases from 28.86 to -6.61 μmol m^{-2} s^{-1}, indicating a reduction in the maximum GPP. Similarly, the mean α decreases from 0.042 to 0.014 mol mol^{-1}, suggesting a decline in the efficiency of light energy utilization for photosynthesis. Additionally, the mean RE_d value decreases from 8.61 to 1.14 μmol m^{-2} s^{-1}, reflecting a decrease in the R_{eco} following conversion. However, the SD of RE_d after conversion was significantly higher at 5.51 μmol m^{-2} s^{-1}, compared to the 1.49 μmol m^{-2} s^{-1} observed before conversion.

Discussion

Changes in environmental conditions

The mean of daily maximum T_{air}_1 above canopy decreased by 0.7°C following conversion (Table 2). However, following the planting of oil palms in May 2018, the mean daily maximum T_{air}_1 was comparable to that of before conversion. Similar pattern was observed in the means of daily minimum T_{air}_1. Hardwick et al. (2015) demonstrated that the effects of LAI on the near-ground microclimate are associated with the amount of solar radiation received by an ecosystem. LAI measured in the PSF from 2011 to 2014 was 7.9 m^2 m^{-2}. Although no LAI measurement was conducted after planting in 2018, LAI is expected to be below 1.0 m^2 m^{-2} for a young palm age (Toh et al., 2017). Before conversion, where

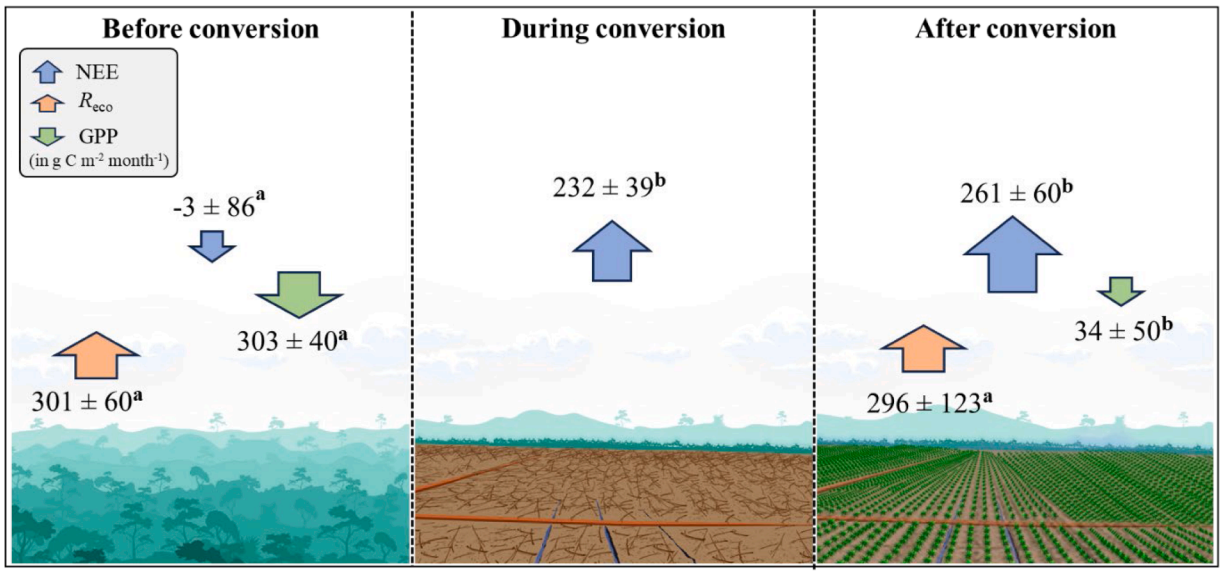

Fig. 5. The comparison between the mean of monthly sum of CO_2 fluxes (mean ± 1SD) in g C m^{-2} month^{-1} across conversion stages. NEE was not partitioned into R_{eco} and GPP for the during conversion period, considering the absence of biomass for photosynthesis. The Tukey's HSD test was used to make pairwise comparisons of the mean values among the three land uses. Downward arrow indicates a net CO_2 sink and upward arrow indicates a net CO_2 source.

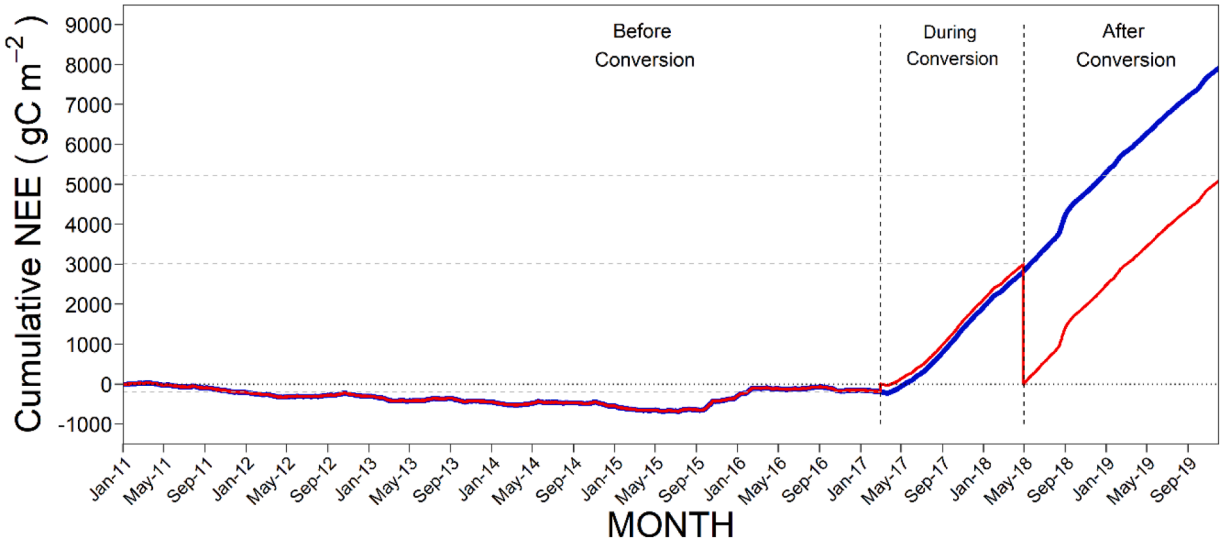

Fig. 6. The cumulative NEE from January 2011 to December 2019. Dotted vertical lines indicate borders between conversion stages. The red line represents cumulative NEE segmented by conversion stages (before, during, and after conversion), while the blue line represents cumulative NEE over the entire period.

the LAI was higher, solar radiation penetrates the plant canopy during the day and is absorbed by and heats the leaves, which increases T_{air}_1 above the canopy. In contrast, similar heating effect was not observed during conversion, as indicated by the decrease in daily maximum and minimum T_{air}_1. The absence of forest biomass during conversion also caused significant loss of water vapor released through transpiration, leading to an increase in daily maximum and minimum VPD_1. Despite an expected reduction in cooling due to decreased plant transpiration during conversion, both the daily maximum and minimum T_{air}_1 decreased. This suggest that the variations in T_{air}_1 were mainly governed by the above canopy local plant temperature. On the other hand, T_{air}_2 (below canopy) was primarily influenced by the vegetation's cover, related to the amount of solar radiation penetrating the canopy (shading), vertical mixing and the cooling effects via transpiration. This is evidenced by the lower mean of daily maximum and minimum T_{air}_2 before conversion, compared to those of T_{air}_1. Although the palm trees could provide a cooling effect similar to that of forest, the T_{air}_2 sensor used in this study was located in an open area, away from the trees. As a result, the observed T_{air}_2 increased by 0.8°C from before to during conversion and further increased by 0.4°C from during to after conversion (after conversion was 1.2°C warmer than before conversion). Similar warming effect after forest conversion was reported by Sabajo et al. (2017). The increase in T_{air}_2 in this study was about 48 % lower than the 2.3°C increase following forest conversion to both rubber plantation and OPP in Jambi province, Indonesia, as reported by Meijide et al. (2018). High spatial variability between open areas and below the canopy is expected in an OPP of this age. Therefore, future research should account for this spatial variability by incorporating measurements from both open areas and below the canopy. Understanding how different canopy cover influence micro-climate conditions will provide a more comprehensive view of temperature dynamics and help refine management practices in OPPs.

The radiation that is not absorbed by the canopy reaches the soil and heats the soil surface. Heat is transmitted down into the deeper soil

Table 4
Correlation analysis between the measured half-hourly nighttime NEE (R_{eco}) and environmental variables using the Pearson correlation coefficient method. Correlation coefficients (r), corresponding p-values, and R-squared values are presented. Significant correlations at the 0.01 level ($p < 0.01$) are indicated by double asterisks (**).

Stage	Variables	*r*	*p*	R^2	n
Before conversion	GWL	-0.06	0.002**	0.004	2737
	VWC_1	-0.05	0.01*	0.002	
	T_{soil}_2	0.06	0.003**	0.003	
	VPD_1	-0.04	0.043*	0.001	
During conversion	T_{air}_1	-0.21	< 0.001**	0.045	775
	T_{air}_2	-0.17	< 0.001**	0.028	
	VPD_1	-0.24	< 0.001**	0.057	
	VPD_2	-0.14	< 0.001**	0.020	
	GWL	0.11	0.002**	0.012	
After conversion	T_{air}_1	-0.09	0.036*	0.007	601
	T_{soil}_2	-0.09	0.031*	0.008	
	GWL	-0.09	0.023*	0.009	
	VWC_1	-0.09	0.026*	0.008	

Table 5
Comparison of light response parameters between two conversion stages (before and after Conversion) using Welch's t-test.

Parameter	Conversion stage	Mean	Degrees of Freedom (df)	t-value	*p* value
P_{max}	Before conversion	28.86	828.56	251.42	***
	After conversion	-6.61			
α	Before conversion	0.042	693.23	46.204	***
	After conversion	0.014			
RE_d	Before conversion	8.61	536.1	32.023	***
	After conversion	1.14			

P_{max}: maximum GPP; α: initial slope (PPFD < 600 μmol m^{-2} s^{-1}); RE_d: dark respiration
*** indicates significance at the 0.001 level.

layers and transferred into the air directly above the soil surface as it warms. As a result, we observed an increase up to 3.6°C in daily maximum of T_{soil} after the conversion compared to before conversion. The exposed bare peat surface after the removal of forest biomass absorbs most of the incoming solar radiation, causing a more substantial increase in T_{soil} rather than an increase in T_{air}. Anamulai et al. (2019) also reported that T_{air} from their study site in OPP was 1.5 – 2.3°C warmer than in PSF. Extreme topsoil heating may also have caused excessive soil drying, as indicated by the increase in midday albedo and low VWC following conversion. In addition, the removal of forest biomass during conversion is also expected to reduce transpiration, which can lead to an increase in surface temperature (Manoli et al., 2018).

Studies have shown that lowering GWL decreases the water-filled pore space (WFPS) and enhances soil aeration (Chaddy et al., 2021; Ishikura et al., 2017). This can significantly reduce soil moisture and increase peat bulk density. Our results showed no significant relationship between VWC and GWL when the GWL was below -40 cm (Fig. 2B&C). This probably indicates that there is a limited effect of capillary action at the uppermost 30 cm of the peat, which is mainly influenced by the depth of the water surface and porosity of the peat. Notably, the VWC measurements in this study were limited to the uppermost 30 cm of the peat soil, and after conversion, the sensor location became exposed to direct sunlight, far from any nearby palm trees. After conversion, high spatial variability of VWC between the open areas and shaded areas near the palm trees is expected. This phenomenon could also be attributed to the drying of topsoil due to the large amount of solar radiation penetrating the soil under open canopy conditions and low GWL.

Changes in CO_2 fluxes

The conversion of PSF to OPP resulted in a significant increase in NEE, shifting the ecosystem from a net CO_2 sink to a net CO_2 source. Monthly NEE increased during conversion primarily due to the loss of GPP following forest biomass removal (Fig. 5). On the other hand, the low GPP after conversion was likely attributed to water stress. Lower mean daily GWL in 2019 (94.1 ± 10.2 cm) probably caused prolonged stress that may have triggered physiological changes in the plant to minimize water loss, such as reduced leaf area and stomatal closure. This scenario could also impair nutrient uptake, and alter metabolic processes of the palm trees, further contributing to the decrease in GPP. Large PT was observed extended from November 2018 to April 2019 (Fig. 2), but GWL remained low at between -80 to -100 cm, likely due to the GWL management by the plantation. The year 2019 also recorded the longest consecutive low monthly PT (6 months) with PT below and slightly over 100 mm $month^{-1}$. The low observed VWC, which was even lower than the during conversion period provides strong evidence of the potential water stress experienced by the oil palm trees. As a result, the annual GPP from 1st January 2019 to 30th December 2019, measured at 373 g C m^{-2} $year^{-1}$, was lower than those reported by McCalmont et al. (2021) for a 16-month-old oil palm in the Sabaju plantation estate, Sarawak (990 ± 740 g C m^{-2} $year^{-1}$). However, our value falls within the 95 % confidence interval of their estimate. This was also 85 % lower than the annual GPP of a mature OPP reported in our previous study (Kiew et al., 2020) and 91 % lower than that of 12-year-old oil palm as reported by McCalmont et al. (2021).

Assuming NEE during conversion is equivalent to R_{eco}, the reduction in R_{eco} during this period may be attributed to decreased plant respiration. While soil respiration and the decomposition of wood debris are likely increased, they did not fully offset for the loss of plant respiration, as indicated by the higher R_{eco} observed before conversion compared to during conversion. After conversion, the planting of oil palm trees led to an increase in monthly R_{eco}, eventually matching the magnitude observed in before conversion ($p > 0.01$). The annual R_{eco} of 3638 ± 255 g C m^{-2} $year^{-1}$ (Table 3) in 2011 to 2016 is comparable to that of the tropical peat swamp forest in Central Kalimantan reported by (Hirano et al., 2012). However, in 2015 and 2016, the average annual R_{eco} was significantly above this value (3823 ± 394 g C m^{-2} $year^{-1}$). This may be attributed to the artifact introduced from the gapfilling, which resulted from prolonged gaps in NEE data between August 2015 and March 2016 due to power supply disruptions. In 2019, the annual R_{eco} decreased significantly to 3116 g C m^{-2} $year^{-1}$, which is approximately 11.6 % lower than that of a mature OPP on peat in the same region (Kiew et al., 2020). Although R_{eco} might be expected to increase after conversion due to elevated peat decomposition associated with the lowering of GWL (Huang et al., 2021), our study showed that there was no significant increase ($p > 0.05$) in R_{eco} (Fig. 5). One possible reason can be the absence of autotrophic living root respiration and domination of heterotrophic respiration, being about 40 % of total peatland forest soil respiration (Hermans et al., 2022). However, dramatic change in water regime is possibly the main reason of R_{eco} dynamics. Although oxidative peat decomposition is expected to increase, further lowering of GWL (maintained below -80 cm following the conversion) could create an excessively dry condition that is not favorable for organic matter decomposition, as demonstrated by Hirano et al. (2014). Likewise, Quan et al. (2019) demonstrated that warming stimulates net C uptake under wet conditions, but depresses it under very dry conditions. McCalmont et al. (2021) reported a higher R_{eco} (5640 g C m^{-2} $year^{-1}$) in an OPP under wetter conditions, where the GWL is maintained at above -60 cm. In addition, lower decomposition might be related to the depth of peat disturbance, affecting the intrinsic recalcitrance of the peat substrate

(Kleber, 2010; Clark et al. 2023). Even if there was an increase in soil respiration following conversion, this may have been offset by a larger loss in plant respiration. In addition, aboveground woody debris is also abundant at the site after land conversion (Hirano et al., 2022). Although the decomposition of woody debris could potentially increase R_{eco}, this effect may have been offset by a reduction in plant respiration. Considering the high magnitude of the loss in plant respiration, this result implies that there was a significant increase in soil respiration and/or aboveground woody debris at the study site. Nevertheless, to explain CO_2 budgets in analogous tropical peatlands conversion sites, detail research is recommended to assess the role of soil respiration and aboveground woody debris.

The mean annual NEE of 2732 ± 655 g C m^{-2} $year^{-1}$ from 2017 to 2019 was 2992 g C m^{-2} $year^{-1}$ and 3680 g C m^{-2} $year^{-1}$ more positive than that of tropical humid evergreen forest (-260 g C m^{-2} $year^{-1}$, Luyssaert et al., 2007) and a 23 year old oil palm on mineral soil (-948 g C m^{-2} $year^{-1}$, Septiwibowo et al. 2019), respectively. Meijide et al. (2020) reported a relatively lower annual NEE during the first year of plantation establishment on mineral soil (1012 ± 51 g C m^{-2} $year^{-1}$). The large increase in annual NEE following conversion was due to an 80 % reduction in GPP; however, R_{eco} only declined by 5 % (Table 3). During the first year of plantation establishment in 2018, which include both during and after conversion period, the annual NEE was 240 % larger than the 7-10 year-old OPP on peat (994 g C m^{-2} $year^{-1}$) reported by Kiew et al. (2020). In 2019 (after conversion), the deficit was reduced to 176 %, primarily due to an 11.6 % and 85.3 % lower annual R_{eco} and GPP, respectively. Hooijer et al. (2012) found decreases in peat decomposition over time following drainage. The annual GPP in 2019 (8 – 19 months old) was lower than that of a 5-16 months old OPP on peat (373 vs. 990 g C m^{-2} $year^{-1}$) reported by McCalmont et al. (2021). Similarly, the annual R_{eco} was 45 % lower (3116 vs 5640 g C m^{-2} $year^{-1}$), resulting in lower annual NEE (2743 vs. 4650 g C m^{-2} $year^{-1}$). The NEE is anticipated to approach zero as GPP increases with palm growth. Our study at another OPP (Kiew et al., 2020), demonstrated that, after 7-10 years, the GPP of oil palm on peat can reach up to 2500 g C m^{-2} $year^{-1}$. However, the severe leaning and toppling of palm trees at this stage of growth may constrain their uptake capacity, thereby impeding GPP. With proper peat compaction, root anchorage can be improved to avoid this problem and be beneficial for palm growth.

Changes in the controlling factors of CO_2 fluxes

The nighttime NEE or R_{eco} exhibited a typical negative relationship with GWL before conversion. However, during conversion, nighttime NEE was negatively correlated with both T_{air} and VPD. Despite a lower correlation coefficient, nighttime NEE significantly increased with GWL during this period ($r = 0.11$, $p < 0.01$). In the absence of GPP after biomass removal, ecosystem CO_2 dynamics were mainly governed by the decomposition of peat and woody debris. This may suggest a potential suppression of peat and woody debris decomposition under dry conditions. Under dry conditions (high T_{air} and VPD), there was a corresponding decrease in VWC or water availability, especially when the GWL was low. Under such conditions, surface soil respiration and aboveground woody debris decomposition are expected to be reduced by desiccation (Hirano et al., 2009). Although Sundari et al. (2012) reported that deeper peat decomposition could increase to offset this reduction, no such effect was observed in this study. This implies a significant influence of both surface soil and aboveground woody debris on the variation in R_{eco} during conversion. On the other hand, the response of nighttime NEE after conversion was comparable to that before conversion, likely due to the shading effect of palm trees and a relatively higher GWL, which retain the soil moisture. These conditions likely prevented excessive drying of the topsoil, which could suppress peat decomposition.

Our results of light response analyses showed that there were significant decreases in P_{max}, α, and RE_d after forest conversion to oil palm plantation. The shift in P_{max} values from positive to negative, observed before conversion and after conversion suggests a significant alteration of the C balance dynamics. This implies that even under light saturated condition, the oil palm plantation is releasing more C through respiration than it is absorbing through photosynthesis. However, study by Stiegler et al. (2019) reported higher P_{max} values (over 25 μmol m^{-2} s^{-1}) in a mature oil palm plantation in Jambi province, Indonesia. The estimated α value from the young plantation in this study was notably lower compared to a previous study (0.014 vs. 0.051 mol mol^{-1}) by Dufrene & Saugier (1993). However, there remains a scarcity of similar studies for direct comparison.

Conclusions

Tropical PSF conversion to OPP released large amounts of CO_2 to the atmosphere on annual basis during conversion. The peatland has remained a large CO_2 source even after the establishment of the OPP in 2018. Young palm age, combined with a low GWL due to prolonged low PT and GWL management in 2019, may have caused the low GPP, that led to the large emission.

The findings of this study highlight the critical role of tropical peatlands in regulating atmospheric CO_2 concentrations. The significant rise in NEE following land-use conversion points to the urgent need for sustainable management practices to mitigate CO_2 emissions. Given that tropical peatlands serve as one of the largest terrestrial carbon stores, their degradation has profound implications for global climate change.

Our results quantify the change in CO_2 dynamics following the conversion of peat swamp forests to oil palm plantation. In conclusion, land conversion resulted in a 2757 g C m^{-2} $year^{-1}$ increase in annual NEE, transforming a previously net CO_2 sink forest ecosystem into a net source of CO_2. This increase in CO_2 emissions was mainly induced by a significant reduction in GPP due to forest biomass removal, as R_{eco} was only slightly reduced following land conversion. The changes in vegetation cover also found to disrupt ecological function and reduce overall ecosystem productivity. During conversion, R_{eco} also did not exhibited the typical relationship with GWL as observed in forest. We speculate that this was primarily due to the extremely dry conditions, as evidenced by the increases in T_{air} and VPD. Therefore, further research is needed to elucidate the long-term impacts of land-use change on ecosystem functions and resilience to environmental stressors. In addition, a complete accounting of other respiration components, such as soil respiration is important in explaining the CO_2 dynamics associated with land-use change.

Given the negative impact of these conversions on global warming, the development of sustainable land management practices that prioritised carbon sequestration and emissions mitigation were vital. For example, emissions could also be reduced through best management practices such as zero-burning policies and maintaining higher water levels in the field, as well as by planting cover crops. Any further conversion of peatlands for oil palm plantations must be done with great caution as the CO_2 emissions would exacerbate global warming.

Data availability

The data utilized in this study are owned by the State Government of Sarawak. Access to these data is restricted and requires official approval from the government. Researchers or other parties interested in obtaining the data are encouraged to submit a formal request to the State Government of Sarawak for approval.

Declaration of generative AI and AI-assisted technologies in the writing process

During the preparation of this work the author(s) used ChatGPT by OpenAI in order to improve the clarity and readability of the manuscript. After using this tool/service, the author(s) reviewed and edited

the content as needed and take(s) full responsibility for the content of the publication.

CRediT authorship contribution statement

Frankie Kiew: Writing – original draft, Visualization, Methodology, Investigation, Formal analysis, Data curation, Conceptualization. **Ryuichi Hirata:** Supervision, Methodology. **Takashi Hirano:** Supervision, Methodology. **Guan Xhuan Wong:** Supervision, Methodology. **Joseph Wenceslaus Waili:** Methodology. **Kim San Lo:** Methodology. **Kaido Soosaar:** Supervision. **Kuno Kasak:** Supervision. **Ülo Mander:** Writing – review & editing. **Lulie Melling:** Validation, Supervision, Resources.

Declaration of competing interest

The authors declare the following financial interests/personal relationships which may be considered as potential competing interests: Frankie Kiew reports writing assistance was provided by University of Tartu. If there are other authors, they declare that they have no known competing financial interests or personal relationships that could have appeared to influence the work reported in this paper.

Acknowledgements

This research was funded in part by the Sarawak State Government and Malaysian Federal Government. We would like to express our gratitude to all supporting staff of Sarawak Tropical Peat Research Institute for their assistance in field work and system maintenance. Lastly, we are grateful to our colleagues and peers for their insightful discussions and constructive feedback throughout the course of this study. This work was also supported by the Estonian Research Council (PRG2032), and the European Union Horizon programme under grant agreement No 101079192 (MLTOM23003R) and the European Research Council (ERC) under grant agreement No 101096403 (MLTOM23415R).

References

Anamulai, S., Sanusi, R., Zubaid, A., Lechner, A., Ashton-Butt, A., Azhar, B., 2019. Land use conversion from peat swamp forest to oil palm agriculture greatly modifies microclimate and soil conditions. PeerJ. 7, e7656. https://doi.org/10.7717/peerj.7656.

Chaddy, A., Melling, L., Ishikura, K., Goh, K.J., Toma, Y., Hatano, R., 2021. Effects of long-term nitrogen fertilization and ground water level changes on soil CO2 fluxes from oil palm plantation on tropical peatland. Atmosphere 12 (10). https://doi.org/10.3390/atmos12101340.

Clark, L., Strachan, I.B., Strack, M., Roulet, N.T., Knorr, K.-H., Teickner, H., 2023. Duration of extraction determines CO$_{2}$ and CH$_{4}$ emissions from an actively extracted peatland in eastern Quebec, Canada. Biogeosciences. 20 (3), 737–751. https://doi.org/10.5194/bg-20-737-2023.

Couwenberg, J., 2011. Greenhouse gas emissions from managed peat soils: is the IPCC reporting guidance realistic? Mires Peat, citeulike-article-id:13916340.

Dargie, G.C., Lewis, S.L., Lawson, I.T., Mitchard, E.T.A., Page, S.E., Bocko, Y.E., Ifo, S.A., 2017. Age, extent and carbon storage of the central Congo Basin peatland complex. Nature 542 (7639), 86–90. https://doi.org/10.1038/nature21048.

Deshmukh, C.S., Susanto, A.P., Nardi, N., Nurholis, N., Kurnianto, S., Suardiwerianto, Y., Hendrizal, M., Rhinaldy, A., Mahfiz, R.E., Desai, A.R., Page, S.E., Cobb, A.R., Hirano, T., Guérin, F., Serça, D., Prairie, Y.T., Agus, F., Astiani, D., Sabiham, S., Evans, C.D., 2023. Net greenhouse gas balance of fibre wood plantation on peat in Indonesia. Nature 616 (7958), 740–746. https://doi.org/10.1038/s41586-023-05860-9.

Dislich, C., Keyel, A.C., Salecker, J., Kisel, Y., Meyer, K.M., Auliya, M., Barnes, A.D., Corre, M.D., Darras, K., Faust, H., Hess, B., Klasen, S., Knohl, A., Kreft, H., Meijide, A., Nurdiansyah, F., Otten, F., Pe'er, G., Steinebach, S., Wiegand, K., 2017. A review of the ecosystem functions in oil palm plantations, using forests as a reference system. Biol. Rev. 92 (3), 1539–1569. https://doi.org/10.1111/brv.12295.

Dufrene, E., Saugier, B., 1993. Gas exchange of oil palm in relation to light, vapour pressure deficit, temperature and leaf Age. Funct. Ecol. 7 (1), 97. https://doi.org/10.2307/2389872.

Furukawa, Y., Inubushi, K., Ali, M., Itang, A.M., Tsuruta, H., 2005. Effect of changing groundwater levels caused by land-use changes on greenhouse gas fluxes from tropical peat lands. Nutr. Cycl. Agroecosyst. 71 (1), 81–91. https://doi.org/10.1007/s10705-004-5286-5.

Gascoin, S., Ducharne, A., Ribstein, P., Perroy, E., Wagnon, P., 2009. Sensitivity of bare soil albedo to surface soil moisture on the moraine of the Zongo glacier (Bolivia). Geophys. Res. Lett. 36 (2). https://doi.org/10.1029/2008GL036377.

Hardwick, S.R., Toumi, R., Pfeifer, M., Turner, E.C., Nilus, R., Ewers, R.M., 2015. The relationship between leaf area index and microclimate in tropical forest and oil palm plantation: Forest disturbance drives changes in microclimate. Agric. For. Meteorol. 201, 187–195. https://doi.org/10.1016/j.agrformet.2014.11.010.

Hermans, R., McKenzie, R., Andersen, R., Teh, Y.A., Cowie, N., Subke, J.-A., 2022. Net soil carbon balance in afforested peatlands and separating autotrophic and heterotrophic soil CO$_2$ effluxes. Biogeosciences. 19 (2), 313–327. https://doi.org/10.5194/bg-19-313-2022.

Hirano, T., Jauhiainen, J., Inoue, T., Takahashi, H., 2009. Controls on the carbon balance of tropical peatlands. Ecosystems. 12 (6), 873–887. https://doi.org/10.1007/s10021-008-9209-1.

Hirano, T., Kusin, K., Limin, S., Osaki, M., 2014. Carbon dioxide emissions through oxidative peat decomposition on a burnt tropical peatland. Glob. Chang. Biol. 20 (2), 555–565. https://doi.org/10.1111/gcb.12296.

Hirano, T., Segah, H., Kusin, K., Limin, S., Takahashi, H., Osaki, M., 2012. Effects of disturbances on the carbon balance of tropical peat swamp forests. Glob. Chang. Biol. 18 (11), 3410–3422. https://doi.org/10.1111/j.1365-2486.2012.02793.x.

Hirano, T., Wong, G.X., Waili, J.W., Lo, K.S., Kiew, F., Aeries, E.B., Hirata, R., Ishikura, K., Hayashi, M., Murata, S., Shiraishi, T., Itoh, M., Melling, L., 2022. Carbon loss from aboveground woody debris generated through land conversion from a secondary peat swamp forest to an oil palm plantation. J. Agric. Meteorol. 78 (4), 137–146. https://doi.org/10.2480/agrmet.D-22-00003.

Hooijer, A., Page, S., Jauhiainen, J., Lee, W.A., Lu, X.X., Idris, A., Anshari, G., 2012. Subsidence and carbon loss in drained tropical peatlands. Biogeosciences. 9 (3), 1053–1071. https://doi.org/10.5194/bg-9-1053-2012.

Houghton, R.A., Goodale, C.L., 2004. Effects of land-use change on the carbon balance of terrestrial ecosystems. Geophysical Monograph Ser. 153, 85–98. https://doi.org/10.1029/153GM08.

Huang, Y., Ciais, P., Luo, Y., Zhu, D., Wang, Y., Qiu, C., Goll, D.S., Guenet, B., Makowski, D., De Graaf, I., Leifeld, J., Kwon, M.J., Hu, J., Qu, L., 2021. Tradeoff of CO2 and CH4 emissions from global peatlands under water-table drawdown. Nat. Clim. Chang. 11 (7), 618–622. https://doi.org/10.1038/s41558-021-01059-w.

Idso, S.B., Jackson, R.D., Reginato, R.J., Kimball, B.A., Nakayama, F.S., 1975. The Dependence of Bare Soil Albedo on Soil Water Content. J. Appl. Meteorol. Climatol. 14 (1), 109–113. https://doi.org/10.1175/1520-0450(1975)014. <0109:TDOBSA>2.0.CO;2.

Ishikura, K., Hirano, T., Okimoto, Y., Hirata, R., Kiew, F., Melling, L., Aeries, E.B., Lo, K. S., Musin, K.K., Waili, J.W., Wong, G.X., Ishii, Y., 2018. Soil carbon dioxide emissions due to oxidative peat decomposition in an oil palm plantation on tropical peat. Agric. Ecosyst. Environ. 254, 202–212. https://doi.org/10.1016/j.agee.2017.11.025.

Ishikura, K., Yamada, H., Toma, Y., Takakai, F., Morishita, T., Darung, U., Limin, A., Limin, S.H., Hatano, R., 2017. Effect of groundwater level fluctuation on soil respiration rate of tropical peatland in Central Kalimantan, Indonesia. Soil Sci. Plant Nutr. 63 (1), 1–13. https://doi.org/10.1080/00380768.2016.1244652.

Jaatinen, K., Laiho, R., Vuorenmaa, A., Del Castillo, U., Minkkinen, K., Pennanen, T., Penttilä, T., Fritze, H., 2008. Responses of aerobic microbial communities and soil respiration to water-level drawdown in a northern boreal fen. Environ. Microbiol. 10 (2), 339–353. https://doi.org/10.1111/j.1462-2920.2007.01455.x.

Kiew, F., Hirata, R., Hirano, T., Wong, G.X., Aeries, E.B., Musin, K.K., Waili, J.W., Lo, K. S., Shimizu, M., Melling, L., 2018. CO2 balance of a secondary tropical peat swamp forest in Sarawak, Malaysia. Agric. For. Meteorol. 248 (July 2017), 494–501. https://doi.org/10.1016/j.agrformet.2017.10.022.

Kiew, F., Hirata, R., Hirano, T., Xhuan, W.G., Aries, E.B., Kemudang, K., Wenceslaus, J., San, L.K., Melling, L., 2020. Carbon dioxide balance of an oil palm plantation established on tropical peat. Agric. For. Meteorol. 295 (September), 108189. https://doi.org/10.1016/j.agrformet.2020.108189.

Kleber, M., 2010. What is recalcitrant soil organic matter. Environ. Chem. 7 (4), 320–332. https://doi.org/10.1071/EN10006.

Laiho, R., 2006. Decomposition in peatlands: reconciling seemingly contrasting results on the impacts of lowered water levels. Soil Biol. Biochem. 38 (8), 2011–2024. https://doi.org/10.1016/j.soilbio.2006.02.017.

Lu, X., Zhang, X., Li, F., & Cochrane, M. A. (2023). *Fire Particulate Emissions from Combined VIIRS and AHI Data for Indonesia, 2015-2020*. ORNL Distributed Active Archive Center. https://doi.org/10.3334/ORNLDAAC/2118.

Luskin, M., Potts, M., 2011. Microclimate and habitat heterogeneity through the oil palm lifecycle. Basic Appl. Ecol. 12, 540–551.

Luyssaert, S., Inglima, I., Jung, M., Richardson, A.D., Reichstein, M., Papale, D., Piao, S. L., Schulze, E.D., Wingate, L., Matteucci, G., Aragao, L., Aubinet, M., Beer, C., Bernhofer, C., Black, K.G., Bonal, D., Bonnefond, J.M., Chambers, J., Ciais, P., Janssens, I.A., 2007. CO2 balance of boreal, temperate, and tropical forests derived from a global database. Glob. Chang. Biol. 13 (12), 2509–2537. https://doi.org/10.1111/j.1365-2486.2007.01439.x.

Malhi, Y., Pegoraro, E., Nobre, A.D., Pereira, M.G.P., Grace, J., Culf, A.D., Clement, R., 2002. Energy and water dynamics of a central Amazonian rain forest. J. Geophys. Res. 107 (D20). https://doi.org/10.1029/2001JD000623. LBA 45-1-LBA 45-17.

Manoli, G., Meijide, A., Huth, N., Knohl, A., Kosugi, Y., Burlando, P., Ghazoul, J., Fatichi, S., 2018. Ecohydrological changes after tropical forest conversion to oil palm. Environ. Res. Lett. 13. https://doi.org/10.1088/1748-9326/aac54e.

McCalmont, J., Kho, L.K., Teh, Y.A., Lewis, K., Chocholek, M., Rumpang, E., Hill, T., 2021. Short- and long-term carbon emissions from oil palm plantations converted from logged tropical peat swamp forest. Glob. Chang. Biol. 27 (11), 2361–2376. https://doi.org/10.1111/gcb.15544.

Meijide, A., Badu, C.S., Moyano, F., Tiralla, N., Gunawan, D., Knohl, A., 2018. Impact of forest conversion to oil palm and rubber plantations on microclimate and the role of the 2015 ENSO event. Agric. For. Meteorol. 252 (January), 208–219. https://doi.org/10.1016/j.agrformet.2018.01.013.

Meijide, A., De la Rúa, C., Guillaume, T., Röll, A., Hassler, E., Stiegler, C., Tjoa, A., June, T., Corre, M., Veldkamp, E., Knohl, A., 2020. Measured greenhouse gas budgets challenge emission savings from palm-oil biodiesel. Nat. Commun. 11. https://doi.org/10.1038/s41467-020-14852-6.

Melling, L., Goh, K. J., Hatano, R., Uyo, L. J., Sayok, A., & Nik, A. R. (2008). Characteristics of natural tropical peatland and their influence on C flux in Loagan Bunut National Park, Sarawak, Malaysia. Proceedings of the 13th International Peat Congress: After Wise Use- The Future of Peatlands, 226–229.

Melling, L., Hatano, R., Goh, K.J., 2005a. Methane fluxes from three ecosystems in tropical peatland of Sarawak, Malaysia. Soil. Biol. Biochem. 37, 1445–1453.

Melling, L., Hatano, R., Goh, K.J., 2005b. Soil CO2 flux from three ecosystems in tropical peatland of Sarawak, Malaysia. Tellus, Series B 57 (1), 1–11. https://doi.org/10.1111/j.1600-0889.2005.00129.x.

Miettinen, J., Hooijer, A., Vernimmen, R., Liew, S.C., Page, S., 2017. From carbon sink to carbon source: extensive peat oxidation in insular Southeast Asia since 1990. Environ. Res. Lett. 12, 24014. https://doi.org/10.1088/1748-9326/aa5b6f.

Page, S.E., Rieley, J.O., Banks, C.J., 2011. Global and regional importance of the tropical peatland carbon pool. Glob. Chang. Biol. 17 (2), 798–818. https://doi.org/10.1111/j.1365-2486.2010.02279.x.

Papale, D., Reichstein, M., Canfora, E., Aubinet, M., Bernhofer, C., Longdoz, B., Kutsch, W., Rambal, S., Valentini, R., Vesala, T., Yakir, D., 2006. Towards a more harmonized processing of eddy covariance CO_2 fluxes: algorithms and uncertainty estimation. Biogeosciences Discussions 3 (4), 961–992.

Quan, Q., Tian, D., Luo, Y., Zhang, F., Crowther, T.W., Zhu, K., Chen, H.Y.H., Zhou, Q., Niu, S., 2019. Water scaling of ecosystem carbon cycle feedback to climate warming. Sci. Adv. 5 (8), eaav1131. https://doi.org/10.1126/sciadv.aav1131.

R Core Team. (2020). *R: A Language and Environment for Statistical Computing*. https://www.r-project.org/.

Reichstein, M., Falge, E., Baldocchi, D., Papale, D., Aubinet, M., Berbigier, P., Bernhofer, C., Buchmann, N., Gilmanov, T., Granier, A., Grünwald, T., Havrankova, K., Ilvesniemi, H., Janous, D., Knohl, A., Laurila, T., Lohila, A., Loustau, D., Matteucci, G., & Valentini, R. (2005). *On the separation of net ecosystem exchange into assimilation and ecosystem respiration: review and improved algorithm*.

Sabajo, C.R., Le Maire, G., June, T., Meijide, A., Roupsard, O., Knohl, A., 2017. Expansion of oil palm and other cash crops causes an increase of the land surface temperature in the Jambi province in Indonesia. Biogeosciences. 14 (20), 4619–4635. https://doi.org/10.5194/bg-14-4619-2017.

Septiwibowo, B., Hadiwijaya, B., Caliman, J.-P., 2019. CO2 balance on oil palm agrosystem in Sumatra, Indonesia. IOP Conf. Ser. 336, 12022. https://doi.org/10.1088/1755-1315/336/1/012022.

Stiegler, C., Meijide, A., Fan, Y., Ali, A.A., June, T., Knohl, A., 2019. El Niño-Southern Oscillation (ENSO) event reduces CO2 uptake of an Indonesian oil palm plantation. Biogeosciences. 16 (14), 2873–2890. https://doi.org/10.5194/bg-16-2873-2019.

Sundari, S., Hirano, T., Yamada, H., Kusin, K., Limin, S., 2012. Effect of groundwater level on soil respiration in tropical peat swamp forests. J. Agric. Meteorol. 68 (2), 121–134. https://doi.org/10.2480/agrmet.68.2.6.

Toh, C.M., Ewe, H.T., Tey, S.H., Tay, Y.H., 2017. A study on leaf area index and SAR image of oil palm with entropy decomposition and deep learning classification. In: *Progress in Electromagnetics Research Symposium, 2017-Novem*, pp. 271–278. https://doi.org/10.1109/PIERS-FALL.2017.8293148.

Ueyama, M., Hirata, R., Mano, M., Hamotani, K., Harazono, Y., Hirano, T., Miyata, A., Takagi, K., Takahashi, Y., 2012. Influences of various calculation options on heat, water and carbon fluxes determined by open- and closed-path eddy covariance methods. Tellus B 64 (1), 19048. https://doi.org/10.3402/tellusb.v64i0.19048.

van Huissteden, J., van den Bos, R., Marticorena Alvarez, I., 2006. Modelling the effect of water-table management on CO2 and CH4 fluxes from peat soils. Geologie En Mijnbouw. https://doi.org/10.1029/2005JG000010. Vermeulen, J., Hendriks, R.F. A., Bepaling van afbraaksnelheden van organische stof in laagveen (1996), Ademhalingsmetingen aan ongestoorde veenmonsters in het laboratorium. Rapport 288, DLO-Staring Centrum (Wageningen)Verville, J.H., Hobbie, S.E., Chapin III, F.S., Hooper, D.U., Response of tundra CH4 and CO2 flux to manipulation of temperature and vegetation (1998) Biogeochemistry, 41, pp. 215-235; Walter, B.P., A process-based, climate-sensitive model to derive methane em.

Waqar, M.M., Sukmawati, R., Ji, Y., Sri Sumantyo, J.T., 2020. Tropical peatland forest biomass estimation using polarimetric parameters extracted from RadarSAT-2 images. Land. 9 (6). https://doi.org/10.3390/LAND9060193.

Yan, W., 2017. A makeover for the world's most hated crop. Nature 543, 306–308. https://doi.org/10.1038/543306a.